The Mechanism of Formation of TiB_2 Particulates Prepared by *In Situ* Reaction in Molten Aluminum

B. YANG, Y.Q. WANG, and B.L. ZHOU

By making use of a novel technique in which TiB_2 particulates are fabricated by an *in situ* reaction in molten aluminum, we have successfully produced TiB_2/Al composites. In order to reveal the characteristic of the technique, the mechanism of formation of TiB_2 particulates obtained by this method is studied in this article. Both theoretical and experimental results have shown that the TiB_2 particulates are formed by a diffusion mechanism when the molar fraction of aluminum in the preform is higher than 43.5 pct. In this case, the TiB_2 particulates are generally spherical, and their mean size is less than 2.0 μm. On the contrary, the TiB_2 particulates are formed by a solution-precipitation mechanism when the fraction is lower than 43.5 pct. In this case, the TiB_2 particulates are multifaceted, and the size of most particulates lies between 3.0 and 6.0 μm.

I. INTRODUCTION

PARTICULATE-REINFORCED light metals have great potential for structure materials due to their high specific strength and modulus. Attempts have been made to enhance the material properties *via* a ceramic second phase of higher strength and higher stiffness. The reinforcing phases and the metal matrix are combined by various processing techniques such as powder metallurgy, preform infiltration, spray deposition, casting technologies, rheocasting, and compocasting.[1–5] These artificial composites have resulted in the realization of strength and modulus goals. However, the composites have rarely been economically viable. Additionally, these processes also have problems such as interfacial reactions leading to undesirable products, thermodynamic and mechanical incompatibility, and internal stresses resulting from the mismatch of thermal expansion coefficients of various phases. Recent studies[6–12] have shown that *in situ* fabrication for producing aluminum matrix composites can produce a new class of naturally stable composites for advanced structural and wear application. More recently, we used a novel technique to generate fine particulates in the parent matrix. This new technique has a number of advantages: (1) the interface is very clean and continuous owing to the fact that the reinforcements are formed by an *in situ* reaction in the parent matrix, and (2) the reaction is typically accomplished at a lower temperature (760 °C to 900 °C) and during very short time, showing that the process is economical. The technique, based on our present investigations, is promising for mass production of aluminum matrix composite by virtue of its low production cost, high production rate, and strong possibility of producing near-net shape parts.

Titanium diboride, which has great potential not only as a refractory material, but also as an electronic material because of its high melting point, hardness, electrical conductivity, and thermal conductivity, has been widely used as a reinforcement phase. So far, no one has studied the mechanism of formation of TiB_2 particulates prepared by *in situ* reaction in molten aluminum. The aim of this study is to elucidate the mechanism of formation of TiB_2 particulates prepared by this method in order to reveal the characteristic of this technique.

The TiB_2 particulates in the composites come from the Ti-B-Al preforms, while investigations on the preforms are relatively convenient; thus, this article will focus on the mechanism of formation of TiB_2 particulates in the preforms.

II. EXPERIMENTAL PROCEDURE

Elemental Ti (99 pct, <75 μm), B (95 pct, <10 μm), and Al (98 pct, <75 μm) were mixed by dry milling for 10 hours in a stainless steel container and balls according to $(1 - X)\ TiB_2 + XAl$ ($X = 5, 30, 40, 80$ wt pct). Then, each powder mixture was mechanically pressed into a cylindrical preform under lower than 100 MPa pressure. The preform was 15 mm in diameter and 20 mm in height. On the other hand, about 700 g commercial pure aluminum was melted in an electric furnace containing a graphite crucible. Then, the preforms were inserted into the molten aluminum held at 1173 K. When all reactions were completed (the end point of the reaction can be determined by observing the evidence of a dazzling light originated from the reacted preform), the preforms were taken out immediately. It is worth noting that the processes mentioned previously were carried out in atmosphere. The products after reaction were characterized by X-ray diffraction (XRD). The morphologies of TiB_2 particulates in the reacted preforms were observed by a Cambridge S360 scanning electron microscope.

B. YANG, Postdoctoral Candidate, is with the Materials Physics and Advanced Composites Department, Institute of Metal Research, Chinese Academy of Sciences, Shenyang 110015, People's Republic of China; also Associate Professor, Department of Materials Science and Engineering, Nanchang University, Nanchang 330029, People's Republic of China. Y.Q. WANG, Professor, is with the Materials Physics and Advanced Composites Department, Institute of Metal Research, Chinese Academy of Sciences. B.L. ZHOU, Professor, is with the Materials Physics and Advanced Composites Department, Institute of Metal Research, and International Center for Materials Physics, Chinese Academy of Sciences.

Manuscript submitted May 28, 1997.

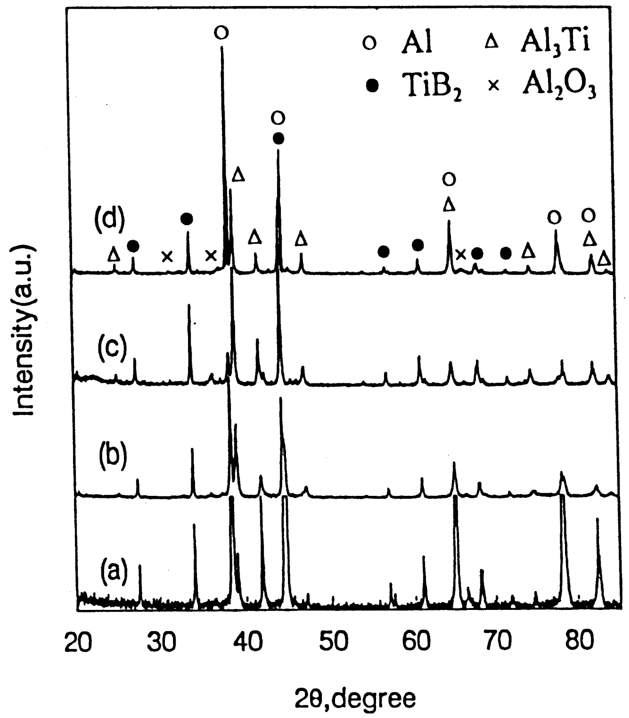

Fig. 1—XRD patterns of the reacted preforms with Ti:B = 1:2 and (*a*) 5.0 wt pct Al, (*b*) 30 wt pct Al, (*c*) 40 wt pct Al, and (*d*) 80 wt pct Al.

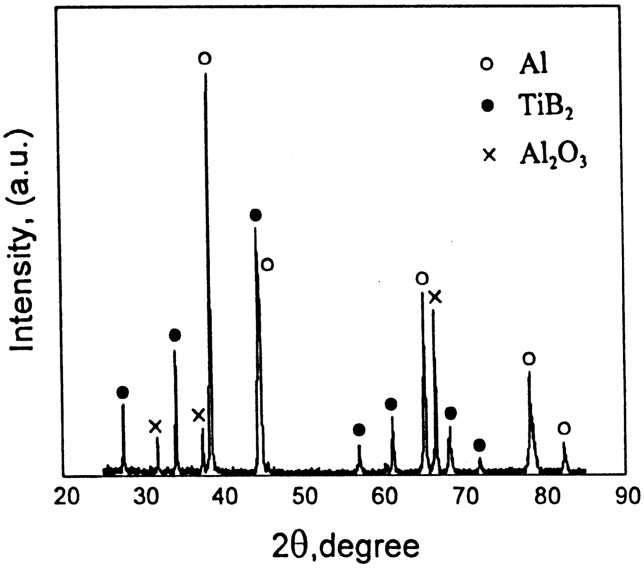

Fig. 2—XRD patterns of the reacted preforms with Ti:B = 1:4 and 40 wt pct Al.

III. RESULTS

A. *Effect of Ti to B Molar Ratio on the Microstructures of the Product Phases*

By means of XRD, the compositions of the phases in the reacted preforms were analyzed, and the experimental results are shown in Figure 1. In addition to the expected presence of TiB_2 and Al peaks, one can see that Al_3Ti and Al_2O_3 peaks are also present in the reacted preforms. Al_2O_3 was not added to the powder mixture and it appears to have been formed during reactions. The mechanism of formation of the Al_2O_3 will be discussed in detail in another article.

The Al_3Ti is observed to be in strip or rectangular structure with a mean size over 20 μm, which is harmful in the plasticity of the composites. The Al_3Ti content increases with increasing titanium content when the aluminum content in the preform is a constant, indicating that the titanium content in the preform with Ti:B = 1:2 is relatively excessive. Thus, another experiment was performed in which the Ti to B molar ratio was 1:4. The compositions of the reacted preform were analyzed by XRD, as shown in Figure 2. One can see that the Al_3Ti is absent in the final product within the precision of the X-ray method. The surface morphology of the reacted preform with Ti:B = 1:4 and 40 wt pct Al is shown in Figure 3. It shows that a number of fine TiB_2 particulates are covered by a thin aluminum layer (Figure 3(a)), which can explain the fact that the wettability between TiB_2 particulates and aluminum is fairly good. The TiB_2 particulates, as indicated in Figure 3(b), close to spheroidicity, and their mean size is about 1.0 μm.

B. *Effect of Aluminum Content on the Morphologies of TiB_2 Particulates*

The morphologies of TiB_2 particulates in the reacted preforms with Ti : B = 1 : 2 and 60 or 5.0 wt pct Al, respectively, are shown in Figure 4. The difference in morphologies of TiB_2 particulates between these preforms is much more significant. The TiB_2 particulates in the former preform are spherical, and their mean size is less than 2.0 μm (Figure 4(a)); while TiB_2 particulates in the latter preform are multifaceted, and their mean size is larger than 3.0 μm (Figure 4(b)). Moreover, some growth steps on the multifaceted TiB_2 particulates can be clearly observed (indicated by an arrow in Figure 4(b)).

It can also be found that, as shown in Figure 5, TiB_2 particulates exhibit different morphologies in different parts of the reacted preform, which contains 5.0 wt pct Al. At the edge of the preform, the TiB_2 particulates are fine and spherical, and their mean size is about 2.0 μm; while in the center of the reacted preform, all of the TiB_2 particulates exhibit larger, multifaceted shapes with a mean size of about 3.0 to 6.0 μm.

IV. DISCUSSION

The standard Gibbs free energy for the possible reactions as a function of temperature when the Ti-B-Al preform is inserted into the molten aluminum is shown[13] in Figure 6. It shows that TiB_2 is thermodynamically very stable. However, as mentioned previously, Al_3Ti was often observed in the reacted preforms, indicating that the titanium atoms react with the molten aluminum when the aluminum powders in the preform are molten and the molten aluminum flows and spreads over the surface of titanium powders. The reaction temperature, in this case, is lower than the melting point of titanium (1953 K); thus, the reaction $3Al_{(l)} + Ti_{(s)} \rightarrow Al_3Ti$ can be written. The reaction is so fast that the heat released by the reaction $3Al_{(l)} + Ti_{(s)} \rightarrow Al_3Ti$ can partially or completely melt the Al_3Ti. The fraction of the molten Al_3Ti, γ', can be obtained by calculation.

Let us assume an infinitely small Al_3Ti system. Considering there is not enough time to dissipate the heat generated by producing the Al_3Ti in the molten aluminum, the

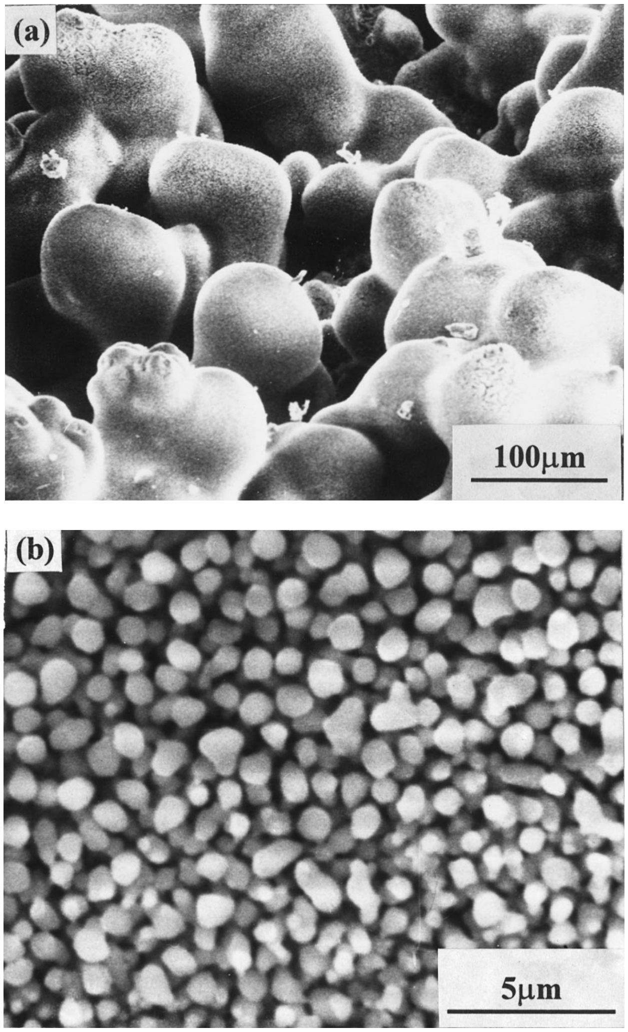

Fig. 3—SEM morphology of the reacted preform with Ti:B = 1:4 and 40 wt pct Al: (*a*) fine TiB_2 particulates covered by a thin aluminum layer; and (*b*) enlarged morphology of (a), showing the morphology of TiB_2 particulates.

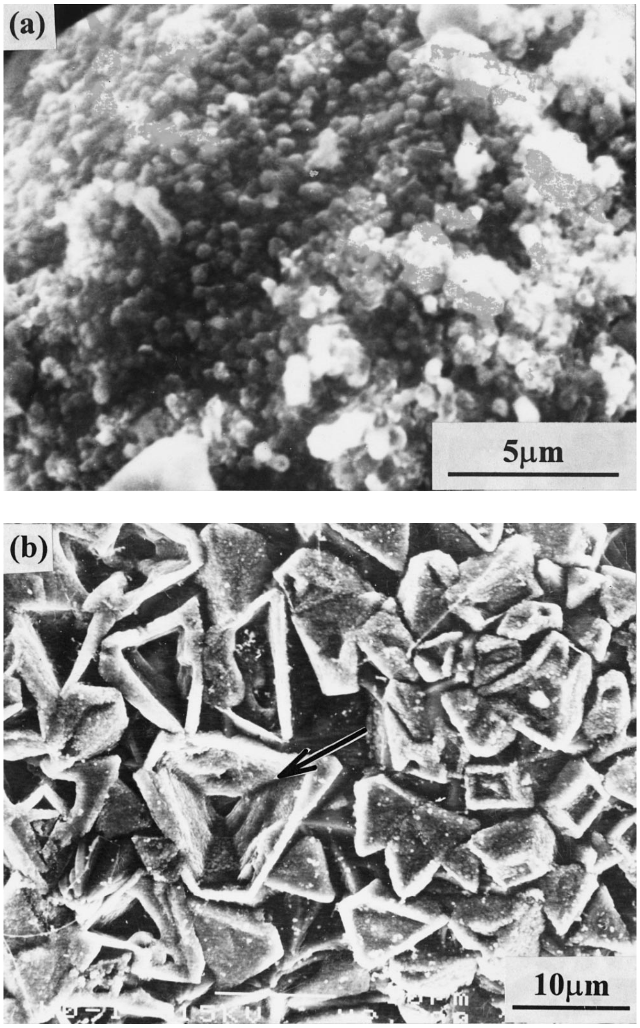

Fig. 4—Morphology of TiB_2 particulates in the reacted preforms with Ti:B = 1:2 and (*a*) 60 wt pct Al and (*b*) 5.0 wt pct Al.

reaction $3Al_{(l)} + Ti_{(s)} \rightarrow Al_3Ti$ goes to the completion, and hence, the system can be regarded as an adiabatic system.

The adiabatic temperature, T_{ad}, can be calculated from the heat balance condition:[9]

$$-\Delta H^0_{T_0} = \int_{T_0}^{T_{ad}} C_p \, dT \qquad [1]$$

where $\Delta H^0_{T_0}$ is the enthalpy of the reaction at T_0 and C_p is the heat capacity of the solid Al_3Ti. The value of T_0 is typically taken as 298 K, and the heat generated by the reaction is the standard heat of formation of the product. In practice, however, the reaction is not initiated at room temperature but at some elevated temperature. This will influence the results. When the elevated temperature is chosen at 1173 K, *i.e.*, the temperature of the molten aluminum into which the preforms are introduced, the fraction of the molten Al_3Ti, γ', will certainly be larger than that of the molten TiB_2 produced at 933 K, *i.e.*, the melting point of aluminum. In order to make the calculated results representative, the T_0 is taken as the melting point of aluminum.

The following equations can be obtained by the preliminary calculations:

$$-\Delta H^0_{f(T_{m,\mathrm{Al}})} > \int_{T_{m,\mathrm{Al}}}^{T_m} C_p \, dT \qquad [2]$$

$$-\Delta H^0_{f(T_{m,\mathrm{Al}})} < \int_{T_{m,\mathrm{Al}}}^{T_m} C_p \, dT + \Delta H_m \qquad [3]$$

where ΔH_m and $\Delta H^0_{f(T_{m,\ \mathrm{Al}})}$ are the enthalpy of fusion of Al_3Ti and the enthalpy of the reaction at the melting point of aluminum, respectively. The term T_m is the melting point of Al_3Ti.

The calculated results show that the heat generated by producing the Al_3Ti makes partial Al_3Ti in the molten condition. Therefore, the Al_3Ti melting point itself is, in this case, the T_{ad}. Based upon the available thermodynamic theory, the following equations can be obtained:

$$-\Delta H^0_{f(T_{m,\mathrm{Al}})} = \int_{T_{m,\mathrm{Al}}}^{T_m} C_{p,s} dT + \gamma' \Delta H_m \qquad [4]$$

$$-\Delta H^0_{f(T_{m,\mathrm{Al}})} = -\Delta H^0_{f(298)} + \int_{298}^{T_{m,\mathrm{Al}}} \Delta C_p \, dt \qquad [5]$$

where $\Delta H^0_{f(298)}$ is the enthalpy of reaction at 298 K, $C_{p,s}$ is the heat capacity of solid Al_3Ti, and γ' is the fraction of molten Al_3Ti.

The thermodynamic data of the Al_3Ti for our calculations are listed in Table I.[13,14] We have $\gamma' \approx 85$ pct from Eqs. [4] and [5].

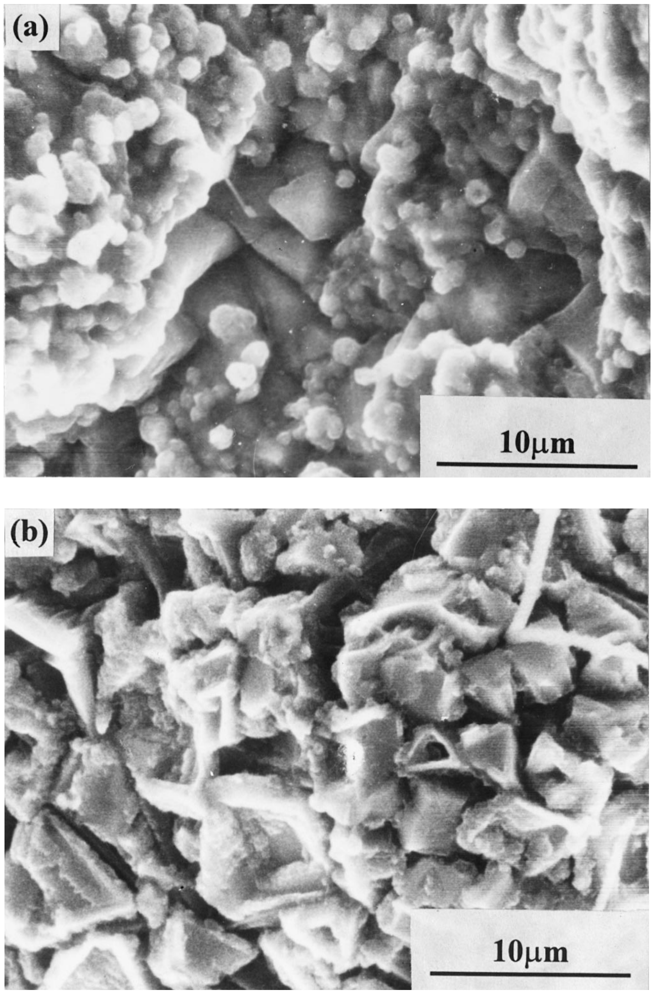

Fig. 5—Morphologies of TiB_2 particulates in different parts of the reacted preforms with Ti:B = 1:2 and 5.0 wt pct Al (*a*) at the edge of the reacted preform and (*b*) in the center of the reacted preform.

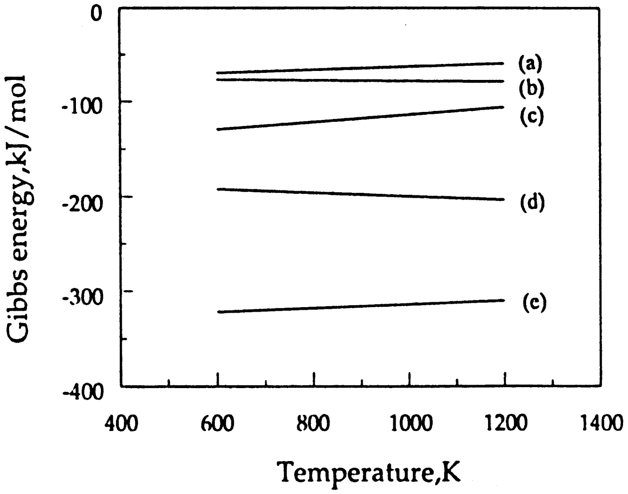

Fig. 6—Standard Gibbs free energy for the possible reactions as a function of temperature when the Ti-B-Al preform is introduced into molten aluminum: (*a*) Al + 2B → AlB_2, (*b*) Al_3Ti + 2Ti → 3TiAl, (*c*) 3Al + Ti → Al_3Ti, (*d*) Al_3Ti + 2B → TiB_2 + 3Al, and (*e*) Ti + 2B → TiB_2.

Table I. Thermodynamic Data of Al_3Ti

Property (Units)	Data
T_m (K)	1613
ΔH_m (kJ mol^{-1})	80
$\Delta H^{\circ}_{f(298)}$ (kJ mol^{-1})	-142.25
$C_{p,s}$ (J k^{-1} mol^{-1})	$103.512 + 16.736 \times 10^{-3}\ T - 8.996 \times 10^{5}\ T^{-2}$
ΔC_p (J k^{-1} mol^{-1})	$-12.774 + 55.631 \times 10^{-3}\ T - 1.82510^{5}\ T^{-2}$ $-62.259 \times 10^{-6}\ T^{2}$

The calculated result shows that about 85 vol pct Al_3Ti produced in the preform is in the liquid state. At this time, the boron atoms can diffuse into the molten Al_3Ti to form some TiB_2 particulates by the reaction Al_3Ti + 2B → 3Al + TiB_2 (also shown in Figure 6). No TiAl was observed in the final reactants, which suggests that the reaction Al_3Ti + 2B → 3Al + TiB_2 is followed by the reaction $3Al_{(l)}$ + $Ti_{(s)}$ → Al_3Ti rather than Al_3Ti + 2Ti → 3TiAl (Figure 6). The reaction Al_3Ti + 2B → 3Al + TiB_2 requires the diffusion of boron atoms into the molten Al_3Ti, showing that the formation of these TiB_2 particulates is controlled by a diffusion process.

The reaction between titanium and boron atoms to form TiB_2 can be expressed as

$$\mathrm{Ti} + 2\mathrm{B} + x\mathrm{Al} \rightarrow \mathrm{TiB_2} + x\mathrm{Al} \qquad [6]$$

where the Al can approximately be treated as all elemental Al powders. This is because the B atoms can, as mentioned previously, diffuse into the molten Al_3Ti produced during the initial stage to form TiB_2-Al solution; *i.e.*, the Al in the Al_3Ti can be returned to the original condition.

When $T_{ad} = T_{m,\mathrm{TiB_2}}$, where T_{ad} is the adiabatic temperature of TiB_2, Eqs. [4] and [5] can be rewritten as

$$\begin{aligned} -\Delta H^{0}_{f(T_m,\mathrm{Al})} = {} & \int_{T_m,\mathrm{Al}}^{T_m,\mathrm{TiB_2}} C_{p,\mathrm{TiB_2}}\, dT + \gamma''\, \Delta H_{m,\mathrm{TiB_2}} \\ & + x \left[\Delta H_{m,\mathrm{Al}} + \int_{T_m,\mathrm{Al}}^{T_b,\mathrm{Al}} C'_{p,l}\, dT \right. \\ & \left. + \Delta H_b + \int^{T_m,\mathrm{TiB_2}}\ _{T_b,\mathrm{Al}}\, C_{p,g}\, dT \right] \end{aligned} \qquad [7]$$

$$-\Delta\ H^{0}_{f(T_m,\mathrm{Al})} = -\Delta\ H^{0}_{f(298)} + \int_{298}^{T_m,\mathrm{Al}} \Delta C_p\, dT \qquad [8]$$

where x is the molar fraction of aluminum; and $\Delta H_{m,\mathrm{TiB_2}}$, $\Delta H^{0}_{f(T_m,\mathrm{Al})}$, and $\Delta H^{0}_{f(298)}$ are the enthalpy of fusion of TiB_2, the enthalpy of the reaction at melting point of aluminum, and the enthalpy of reaction at 298 K, respectively. The term γ'' is the fraction of molten TiB_2. $\Delta H_{m,\mathrm{Al}}$ is the enthalpy of fusion aluminum, T_b is the boiling point of aluminum, $C'_{p,\mathrm{Al}}$ is the heat capacity of liquid aluminum, ΔH_o is the latent heat of vaporization of aluminum, and $C_{p,g}$ is the heat capacity of vapor aluminum.

The thermodynamic data of the TiB_2 and Al for our calculations are listed in Table II.[13,15]

For Al = 5.0 wt pct, we have $\gamma'' \approx 154.33$ pct from Eqs. [7] and [8]. The physical meaning for $\gamma'' > 100$ pct lies in the fact that not only are all of the TiB_2 particulates to be molten in this case, but also the adiabatic temperature (T_{ad}) will exceed the melting point of TiB_2. Therefore, Eqs. [7] and [8] can be rewritten as

Table II. Thermodynamic Data of TiB$_2$ and Al

Property (Units)	Data
TiB$_2$ T_m (K)	3193
ΔH_m (kJ mol^{-1})	83.94
C_{p}, $_{\text{TiB}_2}$ (J k^{-1} mol^{-1})	$56.379 + 25.857 \times 10^{-3}\ T - 17.464 \times 10^5\ T^{-2} - 3.347 \times 10^{-6}\ T^2$
$C_{p,l}$ (J k^{-1} mol^{-1})	108.784
Al T_m (K)	933
ΔH_m (kJ mol^{-1})	10.4
$T_{b,\text{Al}}$ (K)	2450
$C_{p,l}$ (J k^{-1} mol^{-1})	31.748
ΔH_b (kJ mol^{-1})	255.47
$C_{p,g}$ (J k^{-1} mol^{-1})	20.799
$\Delta H^\circ_{f(298)}$ (kJ^{-1} mol^{-1})	-323.8
ΔC_p (J k^{-1} mol^{-1})	$2.129 - 4.427 \times 10^{-3}\ T - 4.912 \times 10^5\ T^{-2} - 3.347 \times 10^{-6}\ T^2$

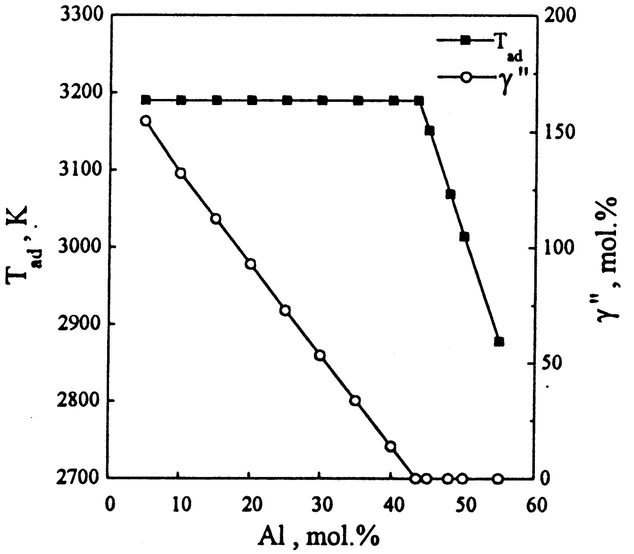

Fig. 7—The influence of the addition of Al as a diluent on the adiabatic temperature and the fraction of molten TiB$_2$.

$$-\Delta\ H^0_{f(T_m,\text{Al})} = \int_{T_m,\text{Al}}^{T_m,\text{TiB}_2} C_{p,\text{TiB}_2}\ dT + \Delta\ H_{m,\text{TiB}_2} + \int_{T_m,\text{TiB}_2}^{T_{ad}} C_{p,l}\ dT + x\left[\Delta\ H_{m,\text{Al}} + \int_{p_m,\text{Al}}^{T_b,\text{Al}} C'_{p,l}\ dT + \Delta\ H_b + \int_{T_b,\text{Al}}^{T_{ad}} C_{p,g}\ dT\right] \qquad [9]$$

$$-\Delta\ H^0_{f(T_m,\text{Al})} = -\Delta\ H^0_{f(298)} + \int_{298}^{T_m,\text{Al}} \Delta\ C_p\ dT \qquad [10]$$

where $C_{p,l}$ is the heat capacity of liquid TiB$_2$. For Al = 5.0 wt pct, we have T_{ad} = 3608 K from Eqs. [9] and [10]. In this case, the molten TiB$_2$ will precipitate from the liquid state during the cooling process in quick succession and grow to be larger TiB$_2$ particulates. The calculated result is confirmed by Figure 4(b), where all of the TiB$_2$ particulates exhibit larger and multifaceted shape.

The effect of the addition of aluminum as a diluent on the theoretical adiabatic temperature (T_{ad}) and on the fraction of molten TiB$_2$ (γ'') is demonstrated in Figure 7. As it can be seen from Figure 7, the fraction of molten TiB$_2$ decreases with increasing aluminum content in the preforms. When the aluminum content reaches and exceeds a critical value, no molten TiB$_2$ can be formed in the reacted preform. For γ'' = 0 in Eq. [7], the critical aluminum content can be achieved; *i.e.*, $x \approx 43.5$ pct. That is, the TiB$_2$ particulates produced in the preforms would only be formed by a diffusion mechanism when the fraction of aluminum is larger than 43.5 pct. On the contrary, there would certainly be some TiB$_2$ particulates formed by a solution-precipitation mechanism in a higher temperature zone. In this article, 5.0 wt pct Al and 60 wt pct Al in the preform were selected. From Figure 4, one can easily find that a lot of larger, multifaceted TiB$_2$ particulates with growth steps exist in the 5.0 wt pct Al preform, showing that the TiB$_2$ particulates are formed by the solution-precipitation mechanism. While all of the TiB$_2$ particulates in the 60 wt pct Al preform are formed by the diffusion mechanism, in this case, their size is fine. It shows that the experimental results are in good agreement with the theoretical calculations mentioned previously.

The theoretical calculation mentioned previously has further been confirmed by another experimental result, as shown in Figure 5. Because the preform is inserted into the molten aluminum, there must exist infiltration of aluminum into the preform, which certainly results in the increase of aluminum content in the preform especially at the edge of the preform. In fact, both phenomena, a flow of liquid aluminum into the porous preform by capillary pressure P_c (plus any applied pressure, P_a) and a diffusion of gas that mainly originated from the reactions among elemental powders through the liquid from the interior where the pressure is higher than that of the surface of the preform, are concurrent. The flow of liquid aluminum due to capillary pressure initially dominates, whereas once the gas within the preform is sufficiently compressed, gas diffusion dominates. The flow of liquid aluminum into a porous preform by capillary pressure can be described by Darcy's law:[16,17]

$$h = \left[\frac{2KP}{\mu(1 - V_p)}\right]^{1/2} t^{1/2} \qquad [11]$$

where h is the infiltrated distance of liquid aluminum during time t,K is the permeability of the porous preform, μ is the viscosity of the liquid aluminum, $P = P_c + P_a - P_i$ (P_i is the opposing internal pressure of the compressed gas), and V_p is the particulate volume fraction. The permeability of a preform is commonly expressed by the Kozeny–Carman equation:[16]

$$K = \frac{D^2\ (1 - \rho)^3}{36C\rho^2} \qquad [12]$$

where D is the mean particulate size, ρ is the relative density, and C is a constant that defines the shape and tortuosity of the pore channels. As the wettability between molten aluminum and the preforms is fairly good, the aluminum content at the edge of the preform with 5.0 wt pct Al can easily exceed 43.5 pct due to the role of the capillary pressure. Therefore, the TiB$_2$ particulates at the edge of the preform will be formed by a diffusion mechanism and grow to be fine particulates. The aluminum content in the center of the preform, however, is also lower than 43.5 pct due to the existence of opposing internal pressure of the compressed gas and the scarcity of the capillary pressure. Thus, the TiB_2 will also be formed by the solution-precipitation mechanism and grow to be a multifaceted structure.

From Figure 6, one can also see that the AlB_2 phase is easy to form. But no AlB_2 has been observed in the final products of the reacted preforms. It is because[18] AlB_2 is only a transition phase. It can be decomposed into AlB_{12} and aluminum at 1200 K, while AlB_{12} can be further decomposed to boron and aluminum at 2400 K (as mentioned previously, the adiabatic temperature is higher than 2400 K during the formation process of TiB_2 particulates). Then boron and titanium atoms can further react with each other to form TiB_2. Thus, the AlB_2 phase does not exist in the final product.

The reason why the Al_3Ti is precluded entirely in the final product when Ti : B = 1: 4 is that the reaction $Ti + 2B \rightarrow TiB_2$ carried out during the final stage can, in this case, take place more completely than if Ti : B = 1 : 2. The heat generated is so high that it can melt all of the Al_3Ti produced during the initial stage. Therefore, the boron atoms can further diffuse into the molten Al_3Ti to form a TiB_2-Al solution (also shown in Figure 6). On the other hand, the Al_3Ti can decompose owing to a large amount of heat liberated to form TiB_2; thus, Al_3Ti is entirely absent in the final product.

In summary, the mechanism of formation of TiB_2 particulates fabricated by *in situ* reaction in molten aluminum can be outlined as follows. (1) the starting aluminum powders are melted when the temperature reaches 933 K and subsequently carry out the reaction $3Al_{(l)} + Ti_{(s)} \rightarrow Al_3Ti$ as soon as the molten aluminum flows and spreads over the surface of titanium powders. The heat liberated by the reaction $3Al_{(l)} + Ti_{(s)} \rightarrow Al_3Ti$ can partially melt Al_3Ti. (2) Then, the reaction $Al_3Ti + 2B \rightarrow 3Al + TiB_2$ takes place after the boron atoms diffuse into the molten Al_3Ti and further liberates heat energy. (3) Finally, the reaction $Ti + 2B \rightarrow TiB_2$ occurs when the temperature in the preform is raised to a critical value. During the entire process, the temperatures in stages (1) and (2) are lower than that in the third stage. The formation of the TiB_2 particulates produced in stages (1) and (2) is controlled by a diffusion mechanism with a relatively slower velocity. The temperature in the third stage is fairly high, and the formation of the TiB_2 particulates produced in this stage depends on the aluminum content in the preform. When the molar fraction of aluminum is larger than 43.5 pct, the TiB_2 particulates will be formed by a diffusion mechanism. On the contrary, there will certainly be some TiB_2 particulates formed by a solution-precipitation mechanism when the fraction of aluminum is lower than 43.5 pct.

V. CONCLUSIONS

The following conclusions can be drawn from the present investigations through studying the formation mechanism of TiB_2 particulates fabricated by *in situ* reaction in molten aluminum.

1. Al_3Ti is always present in the final product when Ti:B = 1:2 and Al = 5.0 to 80 wt pct in the preform. The brittle Al_3Ti phase can be entirely precluded from the final product when Ti:B = 1:4 and Al = 40 wt pct in the preform.
2. The heat liberated by producing the Al_3Ti phase can ignite reaction produced TiB_2.
3. Both theoretical and experimental results have shown that diffusion and solution-precipitation mechanisms occur during the formation process of TiB_2 particulates produced by this method. When the molar fraction of aluminum in the preform exceeds 43.5 pct, the TiB_2 particulates are formed by a diffusion mechanism. In this case, the TiB_2 particulates are generally spherical, and their mean size is about 2.0 μm. While there certainly are some TiB_2 particulates formed by a solution-precipitation mechanism when the fraction of aluminum is lower than 43.5 pct, in this case, the TiB_2 particulates have multifaceted structure, and the size of most them lies between 3.0 and 6.0 μm.

ACKNOWLEDGMENTS

We gratefully thank Messrs. G. Zhou and G.J. Fan for valuable discussions. The financial support provided by the National Natural Science Foundation of China (No. 59431040) is gratefully acknowledged.

REFERENCES

1. P.K. Rohatgi, R. Asthana, and S. Das: *Int. Met. Rev.*, 1986, vol. 31, pp. 115-39.
2. I.A. Ibrahim, F.A. Mohamed, and E.J. Lavernia: *J. Mater. Sci.*, 1991, vol. 26, pp. 1137-56.
3. D.J. Lloyd: *Int. Met. Rev.*, 1994, vol. 39, pp. 1-23.
4. P.K. Rohatgi, S. Ray, R. Asthana, and C.S. Narendranath: *Mater. Sci. Eng. A*, 1993, vol. 162, pp. 163-74.
5. J.T. Burke, C. Yang, and S.J. Canino: *Proc. Conf. on Cast Metal Matrix Composites*, D.M. Stefanescu and S. Sen, eds., American Foundrymen's Society, Inc., Des Plaines, IL, 1994, pp. 141-51.
6. D.A. Hoke, M.A. Meyers, L.W. Meyer, and G.T. Gray: *Metall. Trans. A*, 1992, vol. 23A, pp. 77-86.
7. L. Wang, M.R. Wixom, and L.J. Thompson: *J. Mater. Sci.*, 1994, vol. 29, pp. 534-43.
8. H.A. Grebe, A. Advani, N.N. Thadhani, and T. Kottke: *Metall. Trans. A*, 1992, vol. 23A, pp. 2365-72.
9. Z.A. Munir: *Metall. Trans. A*, 1992, vol. 23A, pp. 7-13.
10. A.R.C. Westwood: *Metall. Trans. A*, 1988, vol. 19A, pp. 749-58.
11. M.K. Premkumar and M.G. Chu: *Metall. Trans. A*, 1993, vol. 24A, pp. 2358-62.
12. M.J. Koczak and M.K. Premkumar: *JOM*, 1993, vol. 45, pp. 44-48.
13. I. Barin and O. Knacke: *Thermochemical Properties of Inorganic Substances*, Springer-Verlag, New York, NY, 1973; I. Barin, O. Knacke, and O. Kubaschewski: *Thermochemical Properties of Inorganic Substances*, Springer-Verlag, New York, NY, 1977, Suppl.
14. D.C. Dunand: *Mater. Manufact. Processes*, 1995, vol. 10, pp. 373-403.
15. P.B. Ross: *Materials Specification Handbook*, E. & F.N. Spon Ltd., London, 1972, p. 3.
16. W.C. Tu and F.F. Lange: *J. Am. Ceram. Soc.*, 1995, vol. 78, pp. 3277-82.
17. A. Alonso, A. Pamies, J. Narciso, C.G. Cordovilla, and E. Louis: *Metall. Trans. A*, 1993, vol. 24A, pp. 1423-32.
18. T. Atoda, I. Higashi, and M. Kobayashi: *Sci. Pap. Inst. Phys. Chem. Res.*, 1967, vol. 61, pp. 92-99.